References and Notes

1. S.-J. Lin, P.-A. Defossez, L. Guarente, *Science* **289**, 2126 (2000).
2. D. K. Ingram *et al.*, *Ann. N.Y. Acad. Sci.* **1019**, 412 (2004).
3. E. J. Masoro, *Exp. Gerontol.* **35**, 299 (2000).
4. R. S. Sohal, R. Weindruch, *Science* **273**, 59 (1996).
5. S. Miwa, K. Riyahi, L. Partridge, M. D. Brand, *Ann. N.Y. Acad. Sci.* **1019**, 388 (2004).
6. R. M. Anderson, K. J. Bitterman, J. G. Wood, O. Medvedik, D. A. Sinclair, *Nature* **423**, 181 (2003).
7. J. Luo *et al.*, *Cell* **107**, 137 (2001).
8. Materials and methods are available as supporting material on *Science* Online.
9. C. L. Goodrick, D. K. Ingram, M. A. Reynolds, J. R. Freeman, N. Cider, *Mech. Ageing Dev.* **55**, 69 (1990).
10. D. P. Kelly, R. C. Scarpulla, *Genes Dev.* **18**, 357 (2004).
11. E. Nisoli *et al.*, *Science* **299**, 896 (2003).
12. D. Larrouy, H. Vidal, F. Andreelli, M. Laville, D. Langin, *Int. J. Obes. Relat. Metab. Disord.* **23**, 1327 (1999).
13. Y. Higami *et al.*, *FASEB J.* **18**, 415 (2004).
14. T. Koshiba *et al.*, *Science* **305**, 858 (2004).
15. D. Bach *et al.*, *J. Biol. Chem.* **278**, 17190 (2003).
16. E. Nisoli *et al.*, *Proc. Natl. Acad. Sci. U.S.A.* **101**, 16507 (2004).
17. C. P. Fenster *et al.*, *Free Radic. Biol. Med.* **37**, 695 (2004).
18. P. Dessi-Fulgheri *et al.*, *Hypertension* **33**, 658 (1999).
19. H. Y. Cohen *et al.*, *Science* **305**, 390 (2004); published online 17 June 2004 (10.1126/science.1099196).
20. F. Picard *et al.*, *Nature* **429**, 771 (2004).
21. E. J. Masoro, B. P. Yu, H. A. Bertrand, *Proc. Natl. Acad. Sci. U.S.A.* **79**, 4239 (1982).
22. S. J. Lin *et al.*, *Nature* **418**, 344 (2002).
23. K. Houthoofd *et al.*, *Exp. Gerontol.* **37**, 1359 (2002).
24. E. Dere *et al.*, *Genes Brain Behav.* **1**, 204 (2002).
25. S. Cook *et al.*, *Swiss Med. Wkly.* **133**, 360 (2003).
26. M. Bluher, B. B. Kahn, C. R. Kahn, *Science* **299**, 572 (2003).
27. C. H. Chiu, W. D. Lin, S. Y. Huang, Y. H. Lee, *Genes Dev.* **18**, 1970 (2004).

28. We thank A. Higgs for help with the preparation of the manuscript, A. Marino for the early experiments of this research, and A. Mejetta for technical assistance. This work was supported by grants from the Ministero dell'Istruzione, dell'Università e della Ricerca cofinanziamento 2003, the Italian Ministry of Health, and the Italian Association of Cancer Research (AIRC).

Supporting Online Material

www.sciencemag.org/cgi/content/full/310/5746/314/DC1
Materials and Methods
Figs. S1 to S3
Table S1
References

21 July 2005; accepted 6 September 2005
10.1126/science.1117728

Sequence Variants in *SLITRK1* Are Associated with Tourette's Syndrome

Jesse F. Abelson,[1,2]* Kenneth Y. Kwan,[3,4]* Brian J. O'Roak,[2]* Danielle Y. Baek,[1,2] Althea A. Stillman,[2] Thomas M. Morgan,[2] Carol A. Mathews,[8] David L. Pauls,[9] Mladen-Roko Rašin,[3] Murat Gunel,[5] Nicole R. Davis,[1,2] A. Gulhan Ercan-Sencicek,[1,2] Danielle H. Guez,[2] John A. Spertus,[10] James F. Leckman,[1] Leon S. Dure IV,[11] Roger Kurlan,[12] Harvey S. Singer,[13] Donald L. Gilbert,[14] Anita Farhi,[7] Angeliki Louvi,[5] Richard P. Lifton,[2,6,7] Nenad Šestan,[3,4] Matthew W. State[1,2,4,6]†

Tourette's syndrome (TS) is a genetically influenced developmental neuropsychiatric disorder characterized by chronic vocal and motor tics. We studied *Slit and Trk-like 1* (*SLITRK1*) as a candidate gene on chromosome 13q31.1 because of its proximity to a de novo chromosomal inversion in a child with TS. Among 174 unrelated probands, we identified a frameshift mutation and two independent occurrences of the identical variant in the binding site for microRNA hsa-miR-189. These variants were absent from 3600 control chromosomes. *SLITRK1* mRNA and hsa-miR-189 showed an overlapping expression pattern in brain regions previously implicated in TS. Wild-type SLITRK1, but not the frameshift mutant, enhanced dendritic growth in primary neuronal cultures. Collectively, these findings support the association of rare *SLITRK1* sequence variants with TS.

TS is a potentially debilitating developmental neuropsychiatric disorder, characterized by the combination of persistent vocal and motor tics, that affects as many as 1 in 100 individuals (*1*, *2*). A substantial portion of clinically referred TS patients also suffer from obsessive-compulsive disorder (OCD), attention deficit hyperactivity disorder (ADHD), or depression (*3*). A TS spectrum of disorders that includes chronic vocal or motor tics as well as tic-related OCD and ADHD is widely recognized. Phenomenological and neurobiological evidence also supports the inclusion of some habit disorders, including trichotillomania (TTM), in this phenotypic spectrum (*4*, *5*).

Several decades of investigation have confirmed a substantial genetic contribution to TS (*6*). Early segregation analyses suggested that the disorder was inherited as a rare, autosomal dominant trait (*7*). However, more recent studies have supported poly- or oligogenic inheritance (*8*). Genome-wide analysis of linkage has implicated intervals on chromosomes 4, 5, 8, 11, and 17 (*9*–*12*), but to date no disease-related mutations have been identified. These investigations have been complicated by a phenotype that typically decreases in severity with age, a high population prevalence of transient tics, and symptoms that overlap with common disorders such as ADHD and OCD (*13*). In addition, marked locus heterogeneity, gene-environment interactions, and the further confounding of assortative mating (*14*, *15*) have all likely hindered gene-mapping efforts.

We focused on a rare subset of TS patients with chromosomal anomalies to circumvent some of these obstacles and identify candidate genes for intensive mutational screening. Such a strategy provides the opportunity to characterize functional sequence variants largely irrespective of their mode of inheritance. We identified a patient presenting with TS and ADHD and carrying a de novo chromosome 13 inversion, inv(13)(q31.1;q33.1) (*16*). There was no family history of tics, TS, OCD, TTM, or ADHD (Fig. 1). Genotyping with multiple short tandem repeat (STR) markers confirmed paternity (*16*) (table S1). The co-occurrence of a de novo chromosomal abnormality with the only known case of TS in the pedigree led us to fine map the rearrangement with the use of fluorescence in situ hybridization (FISH). We found that bacterial artificial chromosomes (BACs) RP11-375K12 and RP11-255P5 span the 13q31.1 and 13q33.1 breakpoints, respectively (Fig. 1, C to F, and table S2).

Three genes map within 500 kilobases (kb) of these two breakpoints (Fig. 1, E and F). Of these, *Slit and Trk-like family member 1* (*SLITRK1*), encoding a single-pass transmembrane protein with two leucine-rich repeat (LRR) motifs in its extracellular domain, was considered the strongest candidate for further study because of its

[1]Child Study Center, [2]Department of Genetics, [3]Department of Neurobiology, [4]Interdepartmental Neuroscience Program, [5]Department of Neurosurgery, [6]Center for Human Genetics and Genomics, [7]Howard Hughes Medical Institute, Yale University School of Medicine, New Haven, CT 06520, USA. [8]Department of Psychiatry, University of California–San Diego, San Diego, CA 92093, USA. [9]Psychiatric and Neurodevelopmental Genetics Unit, Massachusetts General Hospital, Harvard Medical School, Boston, MA 02114, USA. [10]Department of Medicine, University of Missouri–Kansas City, Kansas City, MO 64111, USA. [11]Division of Pediatric Neurology, Department of Pediatrics, University of Alabama at Birmingham, Birmingham, AL 35233, USA. [12]Department of Neurology, University of Rochester School of Medicine, Rochester, NY 14642, USA. [13]Departments of Neurology and Pediatrics, Johns Hopkins University School of Medicine, Baltimore, MD 21287, USA. [14]Division of Neurology, Cincinnati Children's Hospital Medical Center, Cincinnati, OH 45229, USA.

*These authors contributed equally to this work.
†To whom correspondence should be addressed. E-mail: matthew.state@yale.edu

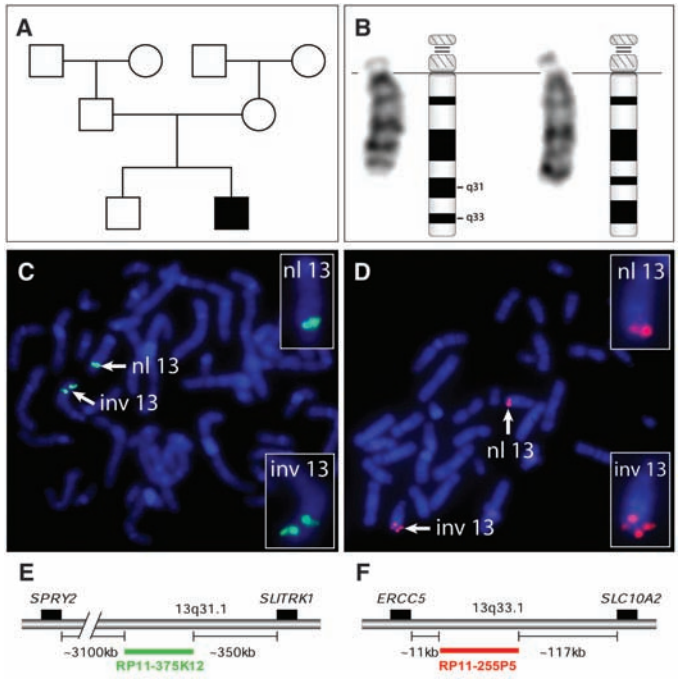

Fig. 1. Mapping of a de novo chromosome 13 paracentric inversion in a child with TS. (**A**) Pedigree of Family 1, with a single affected male child with TS and ADHD (*16*). The parents, grandparents, and younger sibling are not affected with TS, tics, ADHD, TTM, or OCD. Four maternal siblings, not presented on the pedigree, are all unaffected. (**B**) G-banded metaphase chromosomes 13. The ideogram for the normal (left) and inverted (right) chromosomes are presented. (**C** and **D**) FISH mapping of BAC RP11-375K12 (C) and BAC RP11-255P5 (D). The experimental probe is visualized at the expected positions on the normal (nl) chromosomes 13q31.1 and 13q33.1, respectively. Two fluorescence signals are visible on the inverted (inv) chromosomes, indicating that the probes span the breakpoint. Photographs were taken with a 100× objective lens. (**E**) Diagram of the interval surrounding the spanning BAC RP11-375K12 at 13q31.1. *SLITRK1* (National Center for Biotechnology Information accession code NM_052910) maps approximately 350 kb telomeric, and *SPRY2* (NM_005842) maps more than 3 million base pairs centromeric, to the breakpoint. (**F**) Diagram of the interval surrounding the spanning BAC RP11-255P5 at 13q33.1. The gene *ERCC5* (NM_000123.2), mutated in xeroderma pigmentosum group G, maps 11 kb from the spanning BAC clone. The gene *SLC10A2* (NM_000452.1), implicated in primary bile acid malabsorption, maps approximately 100 kb from the spanning BAC clone.

high relative expression in brain regions previously implicated in TS and its suggested role in neurite outgrowth (*17*, *18*). *ERCC5* and *SLC10A2*, mapping immediately centromeric and telomeric, respectively, to the 13q33.1 breakpoint, were not excluded as candidates but were considered less likely alternatives because both have been shown to lead to disorders with no known relationship to TS (*19*, *20*) (Fig. 1F).

The 13q31.1 chromosomal breakpoint mapped well outside the coding region of *SLITRK1*, and direct sequencing of the transcript in the affected individual showed no abnormalities (*16*). Consequently, we hypothesized that the expression of the gene might be altered by a position effect (*21*). However, the genomic organization of the transcript in a single coding exon, in conjunction with its low levels of expression in peripheral lymphocytes, precluded our direct quantitative assessment of *SLITRK1* mRNA in the patient versus controls.

We reasoned, however, that if altered SLITRK1 function contributed to the risk for TS in the patient carrying the inversion, we would expect a subset of TS patients to have mutations in this gene. Accordingly, we screened *SLITRK1* in 174 affected individuals (*16*). We identified one proband, diagnosed with TS and ADHD, who possessed a single-base deletion in the coding region leading to a frameshift, predicted to result in a truncated protein lacking a substantial portion of the second LRR as well as its transmembrane and intracellular domains (Fig. 2).

Four additional family members were ascertained and genotyped (*16*). The mutation

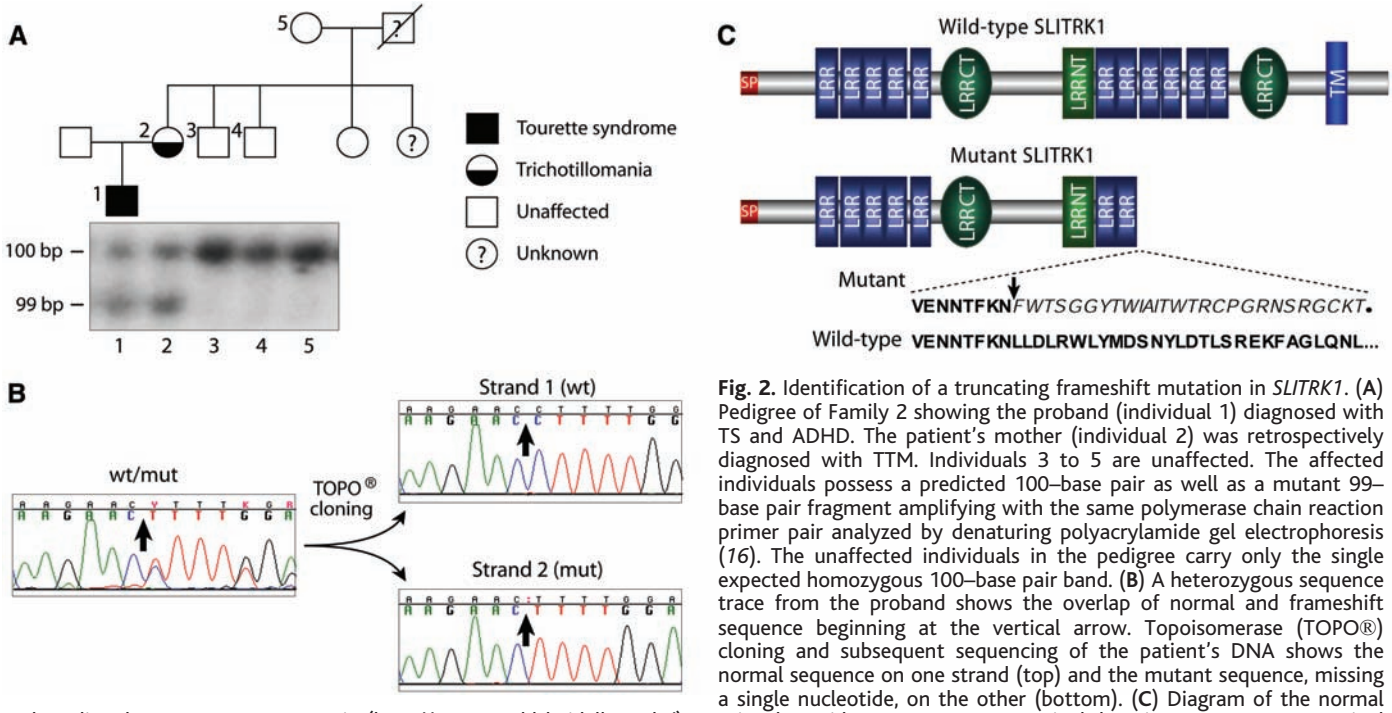

Fig. 2. Identification of a truncating frameshift mutation in *SLITRK1*. (**A**) Pedigree of Family 2 showing the proband (individual 1) diagnosed with TS and ADHD. The patient's mother (individual 2) was retrospectively diagnosed with TTM. Individuals 3 to 5 are unaffected. The affected individuals possess a predicted 100–base pair as well as a mutant 99–base pair fragment amplifying with the same polymerase chain reaction primer pair analyzed by denaturing polyacrylamide gel electrophoresis (*16*). The unaffected individuals in the pedigree carry only the single expected homozygous 100–base pair band. (**B**) A heterozygous sequence trace from the proband shows the overlap of normal and frameshift sequence beginning at the vertical arrow. Topoisomerase (TOPO®) cloning and subsequent sequencing of the patient's DNA shows the normal sequence on one strand (top) and the mutant sequence, missing a single nucleotide, on the other (bottom). (**C**) Diagram of the normal and predicted mutant SLITRK1 protein (http://smart.embl-heidelberg.de/). SP, signal peptide; LRRNT, LRR N-terminal domain; LRRCT, LRR C-terminal domain; TM, transmembrane domain. The predicted amino acid sequence of the mutant protein, showing 27 nonsynonymous substitutions followed by a premature stop codon (•), is presented under the truncated protein diagram and is compared with the wild-type sequence.

was found in the patient's mother, affected with TTM, but not in the two at-risk maternal uncles or in the maternal grandmother, all of whom were unaffected (Fig. 2A). Moreover, the mutation was not present in 3600 control chromosomes (*16*). Finally, no truncating mutations or apparently deleterious variants were identified upon comprehensive mutation screening of the *SLITRK1* coding region in 253 controls (*16*) (table S4).

In addition to this frameshift mutation, the identical noncoding sequence variant (var321) was identified in two apparently unrelated individuals with TS and obsessive-compulsive (OC) symptoms. The single-base change maps to the 3′ untranslated region (UTR) of the transcript and corresponds to a highly conserved nucleotide within the predicted binding site for the human microRNA (miRNA) hsa-miR-189, one of two mature miRNAs derived from the hsa-miR-24 precursor (*22*, *23*) (Fig. 3, A to D, and table S6). This variant was absent from 4296 control chromosomes, demonstrating a statistically significant association with TS ($P = 0.0056$; Fisher's exact test) and raising the question of whether the two occurrences might represent independent genetic events. To evaluate this, we genotyped STRs and single-nucleotide polymorphisms in close proximity to var321. In each case, the variant was found to reside on a distinct haplotype, with distinguishing polymorphisms 83.5 kb centromeric and 3.8 kb telomeric to the variant (table S7), providing strong evidence that the two occurrences arose independently. With a conservative estimate of the mutation frequency at this base ($\sim 10^{-7}$), the likelihood of identifying an independent recurrence of the variant by chance among 346 chromosomes is remote ($P = 0.000056$) (*16*).

DNA samples from the families of both probands carrying var321 were sought. Samples were unavailable from family 3, in which both the mother and father were affected; the mother had a history of chronic motor tics and the father suffered chronic vocal and motor tics, OC symptoms, and hair pulling. In family 4, only the proband carried a formal diagnosis; however, her mother, sister, a maternal grandfather, and a paternal uncle all had a history of tics, subclinical OC symptoms, or both (*16*). DNA was obtained from the immediate family, and its analysis showed that the proband and her mother carried the variant (*16*).

The var321 replaces a G:U wobble base pair with an A:U Watson-Crick pairing at position 9 in the miRNA binding domain. The extent of conservation of this G:U pairing, in both *SLITRK1* 3′UTR and miR-189 (Fig. 3, B and C), as well as evidence that G:U wobble base pairs inhibit miRNA-mediated protein repression to a greater degree than would be expected on the basis of their thermodynamic properties alone (*24*), suggested that var321 might affect SLITRK1 expression. To test this hypothesis, we inserted the full-length *SLITRK1* 3′UTR downstream of a luciferase reporter gene and transfected the construct into Neuro2a (N2a) cells. In the presence of miR-189, the expression of luciferase was significantly reduced (Fig. 3, B to D, and table S8), confirming the functional potential of the mRNA-miRNA duplex. We next inserted the 3′UTR containing var321 and found that the sequence variant resulted in a modest but statistically significant and dose-dependent further repression of luciferase expression compared with that of the wild type (Fig. 3G and table S8).

On the basis of the hypothesis that an altered interaction of *SLITRK1* mRNA with miR-189 contributed to TS in the patients carrying var321, we reasoned that *SLITRK1* and miR-189 expression should overlap in the developing brain. In situ hybridization in postnatal mouse demonstrated that *Slitrk1* mRNA is expressed in the neocortex, hippocampus, thalamic and subthalamic nuclei, striatum, globus pallidus, and cerebellum, in agreement with earlier findings (Fig. 4, A and B) (*17*). We observed mmu-miR-189 expression in the developing neocortex, hippocampus, thalamus, basal ganglia, and cerebellum, overlapping

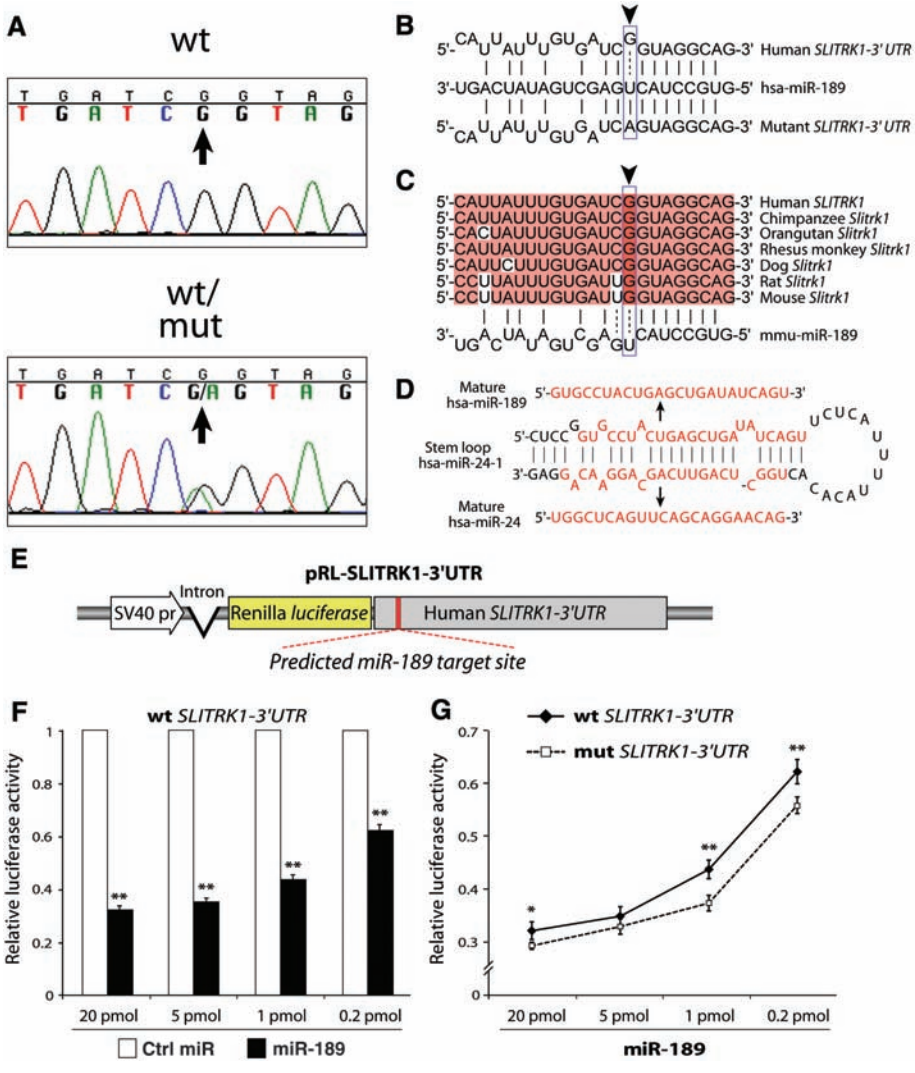

Fig. 3. Characterization and functional analysis of the *SLITRK1* 3′UTR. (**A**) The sequence of the normal 3′UTR and the substitution of G to A found in two probands. (**B**) The substitution maps within a predicted miRNA binding site for miR-189. Base pairing is indicated by a solid (Watson-Crick) or a dashed (wobble) vertical line. (**C**) Conserved bases in the binding domain are shown in red. (**D**) The precursor molecule hsa-miR-24-1 gives rise to hsa-miR-189 and hsa-miR-24. (**E**) pRL-*SLITRK1*-3′UTR contains an SV40 promoter, the *Renilla luciferase* gene, and the full-length 3′UTR of human *SLITRK1*. (**F**) miR-189 and pRL-wt *SLITRK1*-3′UTR, containing the native human sequence, were cotransfected into N2a cells. Relative luciferase activity (*y* axis) versus a random 23–base pair control miRNA. Each experiment was repeated six times for each of four different quantities of miRNA. **, $P = 0.002$ (Mann-Whitney U test). Error bars show maximum values. (**G**) Relative luciferase activity in the presence of miR-189 is shown for the wild-type (wt) *SLITRK1* 3′UTR (solid line) and mutant (mut) *SLITRK1* 3′UTR, containing the substitution of G to A (dashed line). *, $P = 0.009$; **, $P = 0.002$ (Mann-Whitney U test). Error bars show maximum and minimum values.

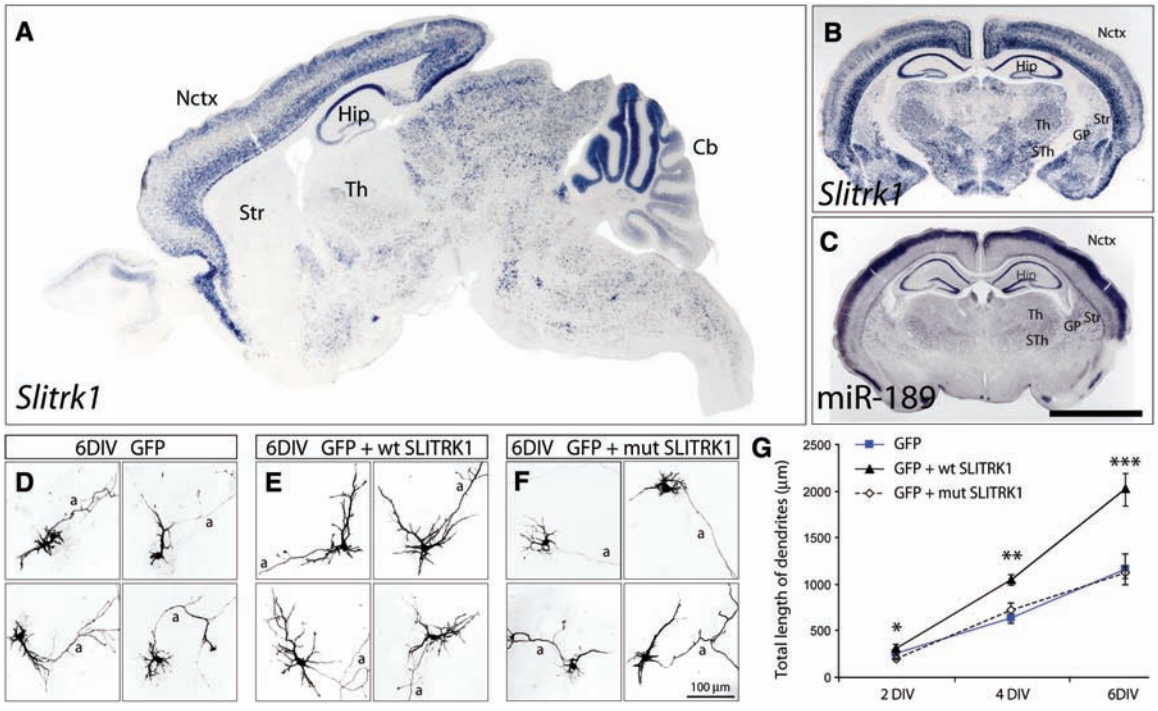

Fig. 4. Overlapping expression of *Slitrk1* mRNA and miRNA-189. (**A** and **B**) *Slitrk1* mRNA is detected in the neocortex (Nctx), hippocampus (Hip), striatum (Str), globus pallidus (GP), thalamus (Th), subthalamus (STh), and cerebellum (Cb) of postnatal day 14 (P14) mouse. (**C**) miR-189 expression is detected in neocortex, hippocampus, and cerebellum at P14. At P9, miR-189 expression is also detected in the striatum, thalamus, and subthalamus (fig. S1). Scale bar, 2 mm. (**D** to **G**) SLITRK1 overexpression enhances dendritic growth in cortical neurons. Images of cell bodies and dendrites, as well as proximal axonal segments (a), of representative GFP-immunopositive cortical neurons cultured for 6 DIV [(D) to (F)]. Primary cultures were prepared from embryonic day 15.5 (E15.5) embryos that were electroporated in utero at E14.5 with control *GFP* plasmid (GFP), *GFP* and wild-type human *SLITRK1* (GFP + wt SLITRK1), or *GFP* and human *SLITRK1* carrying the frameshift mutation (GFP + mut SLITRK1). (G) The total length of dendrites of GFP-immunopositive neurons was measured with the Neurolucida system (*16*) at 2, 4, and 6 DIV. *, $P = 0.002$; **, $P = 0.001$; ***, $P = 0.0007$ (Student's t test for wild-type SLITRK1 versus mutant SLITRK1). Error bars show mean ± SEM.

substantially with *SLITRK1* (Fig. 4C and fig. S1). In fetal human brain at 20 weeks of gestation, we detected *SLITRK1* mRNA in multiple regions, including the developing neocortical plate, subplate zone, striatum, globus pallidus, thalamus, and subthalamus (fig. S2). hsa-miR-189 was highly expressed in the cortical plate and intermediate zone (fig. S2), but not in the basal ganglia or thalamus. Overall, our results demonstrate a developmentally regulated and overlapping pattern of expression of *SLITRK1* mRNA and miR-189 in the neuroanatomical circuits most commonly implicated in TS, OCD, and habit formation (*25*).

Among the six known members of the *SLIT* and *TRK*-like gene family, SLITRK1 is unique in that it lacks tyrosine phosphorylation sites in its short intracellular domain. In this respect, it resembles the SLIT proteins, multifunctional secreted molecules with roles in axon repulsion (*26*) as well as dendritic patterning in the cerebral cortex (*27*). Given the high levels of cortical expression of *SLITRK1*, we investigated its effects on dendritic growth and morphology. Cortical pyramidal neurons were placed in culture after in utero electroporation of mouse embryos with wild-type human *SLITRK1* or the frameshift mutant, along with green fluorescent protein (GFP) (Fig. 4, D to F). At 2 days in vitro (DIV), dendrites expressing wild-type SLITRK1 were significantly longer than those expressing the frameshift ($P = 0.002$; Student's t test). By 4 and 6 DIV, dendrites expressing wild-type SLITRK1 were significantly longer than either comparison group, control or frameshift (Fig. 4G and table S9). These findings resemble, in part, the phenotype elicited by the exposure of cortical neurons to SLIT1 (*27*) and suggest both that SLITRK1 may promote dendritic growth and that the frameshift mutation likely results in a loss of function.

For many complex disorders, the discovery of rare mutations in small subsets of patients has had a major impact in the identification of fundamental pathways that underlie disease pathogenesis. Further study of this new candidate gene, *SLITRK1*, may serve a similar role in the effort to better understand TS at the molecular and cellular level.

References and Notes

1. H. Hornse, S. Banerjee, H. Zeitlin, M. Robertson, *J. Child Psychol. Psychiatry* **42**, 1035 (2001).
2. M. M. Robertson, *J. Psychosom. Res.* **55**, 3 (2003).
3. R. Kurlan *et al.*, *Neurology* **59**, 414 (2002).
4. R. L. O'Sullivan *et al.*, *Biol. Psychiatry* **42**, 39 (1997).
5. J. F. Leckman, *Lancet* **360**, 1577 (2002).
6. D. L. Pauls, *J. Psychosom. Res.* **55**, 7 (2003).
7. D. L. Pauls, J. F. Leckman, *N. Engl. J. Med.* **315**, 993 (1986).
8. J. T. Walkup *et al.*, *Am. J. Hum. Genet.* **59**, 684 (1996).
9. C. Merette *et al.*, *Am. J. Hum. Genet.* **67**, 1008 (2000).
10. P. Paschou *et al.*, *Am. J. Hum. Genet.* **75**, 545 (2004).
11. H. Zhang *et al.*, *Am. J. Hum. Genet.* **70**, 896 (2002).
12. The Tourette Syndrome Association International Consortium for Genetics, *Am. J. Hum. Genet.* **65**, 1428 (1999).
13. H. S. Singer, *Lancet Neurol.* **4**, 149 (2005).
14. R. Kurlan, V. Eapen, J. Stern, M. P. McDermott, M. M. Robertson, *Neurology* **44**, 2336 (1994).
15. P. A. Hanna, F. N. Janjua, C. F. Contant, J. Jankovic, *Neurology* **53**, 813 (1999).
16. Materials and methods are available as supporting material on *Science* Online.
17. J. Aruga, K. Mikoshiba, *Mol. Cell. Neurosci.* **24**, 117 (2003).
18. J. Aruga, N. Yokota, K. Mikoshiba, *Gene* **315**, 87 (2003).
19. P. Oelkers, L. C. Kirby, J. E. Heubi, P. A. Dawson, *J. Clin. Invest.* **99**, 1880 (1997).
20. T. Nouspikel, S. G. Clarkson, *Hum. Mol. Genet.* **3**, 963 (1994).
21. D. A. Kleinjan, V. van Heyningen, *Am. J. Hum. Genet.* **76**, 8 (2005).
22. E. A. Miska *et al.*, *Genome Biol.* **5**, R68 (2004).
23. M. Lagos-Quintana, R. Rauhut, J. Meyer, A. Borkhardt, T. Tuschl, *RNA* **9**, 175 (2003).
24. J. G. Doench, P. A. Sharp, *Genes Dev.* **18**, 504 (2004).
25. H. S. Singer, K. Minzer, *Brain Dev.* **25** (suppl. 1), S70 (2003).
26. K. Brose *et al.*, *Cell* **96**, 795 (1999).
27. K. L. Whitford *et al.*, *Neuron* **33**, 47 (2002).

28. Funded by NIH grants NINDS-R01 NS43520, NCRR-K23 RR16118 and an institutional grant from the Howard Hughes Medical Institute (M.W.S.), NINDS-R01 NS054273 (N.S.), awards from the Shepherd Foundation and the Lawrence Family (M.W.S.), and a Natural Sciences and Engineering Research Council postgraduate scholarship (K.Y.K.). We thank the additional members of the Yale Tourette Syndrome Pediatric Autoimmune Neuropsychiatric Disorders Associated with Streptococcal Infections (PANDAS) Consortium: R.A. King, B. Coffey, P. J. Lombroso, E. Kaplan, and P. Como; S. Hannigen, H. Grantz, L. Katsovich, D. Pendley, C. Drazinic, C. Nelson-Williams, J. J. Miller, J. Garoza, N. Lifton, B. Levy, M. Pappy, and L. Golovyan for their assistance; S. Levi Pearl of the Tourette Syndrome Association and the Tourette Syndrome Association International Consortium for Genetics; and the participating patients and families, without whom this work would not have been possible.

Supporting Online Material

www.sciencemag.org/cgi/content/full/310/5746/317/DC1
Materials and Methods
SOM Text
Figs. S1 and S2
Tables S1 to S9
References

23 June 2005; accepted 20 September 2005
10.1126/science.1116502

Supporting Online Material for

Sequence Variants in *SLITRK1* Are Associated with Tourette's Syndrome

Jesse F. Abelson, Kenneth Y. Kwan, Brian J. O'Roak, Danielle Y. Baek, Althea A. Stillman, Thomas M. Morgan, Carol A. Mathews, David L. Pauls, Mladen-Roko Rašin, Murat Gunel, Nicole R. Davis, A. Gulhan Ercan-Sencicek, Danielle H. Guez, John A. Spertus, James F. Leckman, Leon S. Dure IV, Roger Kurlan, Harvey S. Singer, Donald L. Gilbert, Anita Farhi, Angeliki Louvi, Richard P. Lifton, Nenad Šestan, Matthew W. State*

*To whom correspondence should be addressed. E-mail: matthew.state@yale.edu

Published 14 October 2005, *Science* **310**, 317 (2005)
DOI: 10.1126/science.1116502

This PDF file includes:

Supporting Online Material

A. Clinical Information

Family 1: The family was recruited and evaluated under an approved institutional review board (IRB) protocol at the University of California-San Diego. The proband (proband 1) is a Caucasian boy with a history of tics beginning at age 2, consisting of eye blinking and head turning, followed by shoulder shrugs lasting a few months. He was diagnosed with TS at age 3 due to a full body tic that his parents mistook for a seizure. An electroencephalogram performed at that time was normal. The patient's subsequent history included multiple facial, shoulder and head tics, and some "just-right" behaviors. He also had a history of coughing, throat clearing, sniffing, echolalia and palilalia. The patient was evaluated by one of the authors (CAM) at 6 years of age. At that time, on the Yale Global Tic Severity Scale (YGTSS) his "worst ever" scores were 11/25 for motor and 8/25 for vocal tics, yielding a "worst ever" total tic score of 19/50, which places him in the mild to moderate range of severity. Based on a standardized research evaluation, the patient was diagnosed with definite TS, mild intensity, and attention deficit hyperactivity disorder (ADHD), combined type, moderate intensity. He had no significant obsessive-compulsive (OC) symptoms and no other psychiatric diagnoses.

The patient had previously been diagnosed with a de novo chromosome 13 inversion found incidentally on prenatal testing performed because his mother was a carrier for an unrelated disorder. The mother was noted to smoke 1 pack of cigarettes per day during pregnancy, but there were no other known exposures in utero. His early developmental history was unremarkable. He was the product of a normal spontaneous

delivery at 38 weeks and reached his developmental milestones in the first years of life as expected, with the exception of a slight delay in fine motor skills, which were thought to be normal at the time of the 6-year exam. There was no evidence of mental retardation or learning disability.

The patient's past medical history was otherwise unremarkable based on parental report. There was no history of biliary malabsorption, excessive sun sensitivity, or cancer. On physical exam, there was no evidence of dysmorphology or concurrent medical illness.

The patient's parents were evaluated as part of the research study and neither met diagnostic criteria for TS, tics, TTM (trichotillomania), ADHD or obsessive compulsive disorder (OCD). There was a history of ADHD reported in a maternal cousin. There was no history of tics, TS, TTM, or OCD in the extended family.

Family 2: The family was recruited and evaluated under an approved IRB protocol at the Yale University School of Medicine. The proband (proband 2) is a Caucasian male diagnosed with ADHD, combined type, by his pediatrician at 5 years of age, and was given a clinical diagnosis of TS at age 6. He was initially evaluated in the Yale Tic Specialty clinic at age 10 as a participant in longitudinal studies related to the pathogenesis of TS.

At the time of the initial research evaluation, the patient's family reported that his "worst ever" tics were experienced between the ages of 5 to 6 years. By history, he

received a YGTSS total tic score of 24 out of 50 suggesting moderate symptoms. He exhibited both simple and complex motor tics including eye blinking, turning up the corner of his mouth, jaw stretching, lifting his chin up, side-to-side and up-and-down head movements, and kicking out his leg when sitting. His vocal tics included throat clearing and tongue clicking. Based on consensus research criteria, he was diagnosed with definite TS and definite ADHD, combined type.

The proband's past medical history was notable for a head injury with loss of consciousness at 6 years of age. This injury was subsequent to the onset of both ADHD symptoms and the clinical recognition of tics. He suffered multiple ear infections, and was status-post myringotomy at age 2.

The patient's early developmental history was unremarkable. There were no pre- or peri-natal complications and he met his developmental milestones appropriately. There was no evidence of mental retardation.

The family history was remarkable for hair pulling by the patient's mother beginning in childhood and continuing to the present day. She first developed symptoms of pulling scalp hair, eyebrows and eyelashes in her early teens. She developed a bald spot and was given a wig to wear at school to avoid ridicule. She recalls that her symptoms were most severe during adolescence and resulted in "wiping out" her eyebrows and eyelashes during that period of time. The hair pulling and consequent hair loss resulted in significant distress when the symptoms were at their peak. She was brought to medical attention by her parents for her symptoms. Since adolescence, her symptoms continued with a waxing and waning course, though overall the intensity was

reported to have decreased with time, except during periods of stress. She did not report experiencing a rising sense of tension prior to the pulling of her hair, but did note "just-right" sensations involving the identification of the "correct hair" to pull and relief when completing the act. She had never suffered from other abnormal movements or vocalizations. She denies any current symptoms of OCD and denies any history of ADHD.

The proband's maternal grandfather was deceased and it was recalled that he had a "facial tic" by some family members which consisted of chewing the inside of his cheek. The maternal grandmother had no history of TS-spectrum conditions. Neither maternal uncle carried a history of TS, ADHD, OCD or tics. One maternal aunt was assigned affected status unknown as she declined evaluation and participation in the genetic study. A second maternal aunt agreed to be interviewed and was asymptomatic with no history of ADHD, tics, OCD or TS. However, she subsequently declined participation in the genetic study.

Family 3: The proband is a Caucasian male who originally developed motor tics at age 9 that consisted of head jerks and facial grimaces. He reported the onset of nose twitching, arm flexing and foot stomping at age 10. He subsequently developed vocal tics that included coughing, throat clearing, sniffing and making "animal noises." He was seen clinically for these difficulties at age 14, noted significant distress as a consequence of the chronic symptoms, and was given a diagnosis of TS.

During his initial evaluation for research participation at age 15, the patient was noted to have eye blinking, facial grimaces, unusual mouth movements and shoulder shrugging. His vocal tics on presentation consisted of grunting, squeaking and snorting. His YGTSS total tic score at initial evaluation was 30 of 50 suggesting moderate symptoms.

The patient denied significant obsessions at the time of the evaluation, but did acknowledge a past history of repeated lock checking, a preoccupation with symmetry and exactness and staring rituals. His OC symptoms were considered "slight." He received a research consensus diagnosis of TS with OC symptoms.

His past medical history was unremarkable with the exception of mild asthma for which he used an inhaler and a history of chronic sinusitis. There was no history of recurrent streptococcal infection.

His developmental history was reportedly unremarkable. There was no evidence of mental retardation or learning disability.

The patient’s family history was positive for tics in both parents. The mother reported that as a child she had symptoms similar to those observed in her son. During the proband's initial research evaluation, she was noted by the examiner to have multiple facial tics, but she did not undergo additional diagnostic evaluation.

The patient’s father had a long history of vocal and motor tics. He developed tongue biting and chewing at age 9 along with shoulder shrugging and tensing, knee bending, and joint cracking. He continued to have tics of "moderate forcefulness" into adult life and reported only occasional periods of going without motor tics. He noted

developing a need to pull the hair on his scalp beginning at age 11 that persisted into adulthood. The only reported vocal tic was throat clearing that developed at age 11 which continued through childhood but was described as absent in adult life.

The patient's father also noted mild OC symptoms beginning at approximately age 9 including preoccupations with ordering and arranging and counting compulsions. In adulthood he noted obsessions with saving papers, feeling that he needed to pray "excessively" and needing to "even things up." His OC symptoms caused no reported distress.

Family 4: The patient is a Caucasian female evaluated at age 7 for a several year history of throat clearing, shoulder shrugging and eye-blinking. Based on these symptoms and her distress, she was given a clinical diagnosis of TS. She was subsequently enrolled in a multi-center study of TS and underwent research consensus diagnostic evaluation which confirmed the diagnosis and demonstrated she suffered from mild OC symptoms. These consisted of intrusive thoughts that required her to eat only certain foods and in a specific order. She also reported a preoccupation with ordering and arranging.

The patient's past medical history was uneventful. There was no history of head trauma, seizure, neurological disorder or recurrent streptococcal infection. Her developmental history was unremarkable, with no evidence of mental retardation or learning disability.

No one else in the family carried a formal diagnosis in the TS-spectrum. However, the patient's mother reported that the proband's sister had suffered from

transient throat clearing as a child and, during periods of stress, had what the mother felt was an eye-blinking tic. By history, a paternal uncle suffered from life-long throat clearing and markedly excessive hand washing. The maternal grandfather demonstrated the identical food preoccupations as those identified in the proband, involving ordering and arranging, a need to eat foods one at a time and a marked distain for foods touching each other. The patient's mother noted that she suffered from mild intrusive thoughts including an inability to walk under ladders as well as a preoccupation with hand washing. She noted that these concerns, while not impairing, were ego-dystonic and she felt the need to perform repetitive actions to ward off a negative consequence if she violated one of these “superstitions.”

B. Materials and Methods

TS Sample: 174 probands were comprehensively screened for mutations in the coding region of *SLITRK1*. These were drawn from a total of 202 available samples. 27 samples could not be completed due to poor quality or low quantity of DNA. Males accounted for 78.1% of the sample. Self-described ethnic data were available for 171 of the 174 patients: 93.0% Caucasian, 2.9% Hispanic, 2.9% African-American, and 1.2% Asian. 139 patients were comprehensively screened for variations in 3' UTR of *SLITRK1*. Males accounted for 79.1% of the sample. Ethnic data was available for 136 of the 139 patients: 93.4% Caucasian, 2.9% Hispanic, 2.2% African-American, and 1.5% Asian.

Control Sample: Controls for mutation screening and SNP genotyping were drawn randomly from a group comprised of 2188 ethnically heterogeneous anonymized DNA samples derived from an unrelated project involving acute coronary syndrome (1134 cases/1054 controls). Males accounted for 65.2% of the samples. The self-identified racial distribution was 82.9% Caucasian, 13.6% African-American, and 3.5% other races.

Fluorescence in situ hybridization (FISH)

Studies were undertaken to fine map the chromosome 13 inversion, inv(13)(q31;q33), using FISH as previously described (*S1*). Bacterial artificial chromosomes (BACs) corresponding to regions predicted to contain both breakpoints were identified in the May 2004 assembly at the UCSC Genome Browser (http://genome.ucsd.edu) and obtained from the Roswell Park Cancer Institute (RPCI-11)

library (table S2). BACs were cultured overnight and DNA was extracted using NucloBond Plasmid Midi Kit (BD Biosciences, San Jose, CA). Probes were hybridized to metaphase spreads to confirm both the centromeric and telomeric extent of each breakpoint. BACs within these intervals were then successively hybridized until overlapping clones were identified as centromeric, spanning, and telomeric to each breakpoint (table S2).

Amplification of *SLITRK1*

Genomic sequence for the 5' UTR, coding region, and 3' UTR of *SLITRK1* were obtained from the UCSC Genome Browser. Primers flanking amplicons between 400 and 600 base pairs were designed using Primer3 software (http://frodo.wi.mit.edu/cgi-bin/primer3/primer3_www.cgi) with a minimum overlap of 50 base pairs in order to ensure high quality sequence across the amplified interval (table S3). PCR amplification was performed in 96/384-well plates, using 50 ng DNA as template in a 20μl reaction. The standard reaction mixture contained 10μl 2x FailSafe™ Buffer Premix D (Epicentre, Madison, WI), 1μl 10μmol of each primer, 0.05μl cloned Pfu DNA polymerase (Stratagene, La Jolla, CA), and 0.45μl Taq DNA polymerase isolated from an E. coli strain that carries the DNA polymerase gene from T. aquaticus.

Two PCR cycling protocols were used: a standard protocol and an alternate touch down protocol (TD) for difficult to amplify regions. The standard protocol was comprised of a denaturation step at 95°C for 4 min, followed by 30-35 cycles of a 95°C denaturation step for 30 sec, an annealing step at an optimized temperature (table S3) for

30 sec, and a 45 sec extension step at 72°C. The reaction was completed with a 10 min extension step at 72°C. The touch down (TD) protocol was as follows: Step 1: (1x) 95°C for 4 min; Step 2: (30X) 95°C for 30 sec, 60°C (minus 0.1°C per cycle) for 30 sec, 72°C for 45 sec; Step 3: (5X) 95°C for 30 sec, 56.8°C for 30 sec, 72°C for 45 sec; Step 4:(1X) 72°C for 10min.

Temperature Gradient Capillary Electrophoresis

After PCR amplification, test samples were mixed 1:1 with a sequenced homozygous control and diluted 1:10 with 1X PCR buffer (Roche, Indianapolis, IN). Mixing with a known control allows for the identification of both heterozygous and homozygous mutations. Samples were covered with ~20μl of mineral oil to prevent evaporation and were then denatured and slowly cooled to facilitate heteroduplex formation, using the following protocol: 3 min at 95°C, 95°C-80°C ramp at 3°C/min, 80°C-50°C ramp at 1°C/min, 50°C hold for 20 min, 50°C-45°C ramp at 1°C/min, 45°C-25°C ramp at 2°C/min, cool and hold at 4°C. After heteroduplex formation, sample plates were centrifuged at 2000 rpm for 2 min and then stored at 4°C until needed.

Samples were analyzed using a Spectrumedix 96-capillary Reveal Mutation Discovery System (Spectrumedix, State College, PA). Samples were run over 50-60°C temperature gradient using the manufacturer's recommended procedures. The temperature gradient ramp time was estimated based on the size of the amplicon using the Spectrumedix Chemistry Guide. Data were transformed and analyzed using the bundled Revelation software 2.4 (Spectrumedix). Electropherograms from samples were

compared to a known homozygous control and a mutation score was calculated by the software based on divergence from the control. A score of >50 for potential mutants is recommended by the manufacturer, and we elected to use the following cutoffs to ensure high sensitivity detection: a score of <30 was classified as non-mutant, 30-90 as undecided, and >90 as mutant. Samples with multiple peaks were scored undecided (regardless of score). Both undecided and putative mutant samples were sequenced on one strand at Genaissance Pharmaceuticals (New Haven, CT).

The sequence was analyzed using Sequencher software (Genecodes, Ann Arbor, MI). All possible variants were sequenced on the complementary strand. Sequence variations of interest were confirmed further by SNP genotyping, TOPO cloning of the individual strands, and/or denaturing polyacrylamide gel electrophoresis. Non-synonymous sequence variants were evaluated with PolyPhen (http://www.bork.embl.heidelberg.de/PolyPhen/) and SIFT (http://blocks.fhcrc.org/sift/SIFT_seq_submit2.html).

Genotyping with Short Tandem Repeat (STR) Markers

Paternity was confirmed using selected STR markers from the ABI PRISM ® Linkage Mapping Set V. 2.5 (Alameda, CA). To test for a common haplotype in the region surrounding *SLITRK1*, additional STR markers were generated by querying the human genome sequence using the UCSC Genome Browser. BACs in the region of interest were evaluated for repeats containing at least 18 dinucleotide pairs. Primers flanking these potential markers were designed using Primer3 software and one primer

from each pair was labeled with either 5-Carboxyfluorescein (5-FAM) or 6-Hexachlorofluorescein (HEX) during synthesis. PCR amplifications were performed using the standard PCR reaction noted above, with a 55°C annealing temperature. Amplified samples were sent to W.M. Keck Foundation Biotechnology Resource Laboratory (New Haven, CT) for analysis. Genotypes were called manually using GeneMapper® Software V. 3.7 (Applied Biosystems, Foster City, CA).

All tested markers were consistent with reported paternity in families 1 and 4 (table S1). Informative markers for the var321 haplotype analysis and their genomic locations are listed in table S7. The haplotype shared by the mother and daughter carrying var321 in family 4 was determined and compared to both alleles for proband 3, given the unavailability of parental DNA in family 3. Primer sequences are available upon request.

Statistical Analysis of var321

We sought to determine the probability of independently observing an identical var321, given the null hypothesis of no association with TS and controlling for mutation screening of all relevant sites in the *SLITRK1* gene. We specified a mutation frequency characteristic of CpG dinucleotide sites (1.6 x 10E-7) (*S2*), of which there are 158 in the entire *SLITRK1* transcript including 5 and 3' UTRs. Given the first var321, the conditional probability of a second observation in 346 subsequent alleles is: $1-(1-1.6\text{x}\ 10\text{E-}7)^{346} = 5.5\ \text{x}10\text{E-}5$.

TOPO® Cloning

To confirm the single base deletion and resulting frameshift mutation, amplification of Proband 2 DNA was undertaken with CD-5 primers (table S3). The PCR product was gel extracted, purified, and then cloned with the TA Cloning® Kit (Invitrogen, Carlsbad, CA). Clones were sequenced on both strands at the W.M. Keck Foundation Biotechnology Resource Laboratory.

As part of our analysis of haplotypes surrounding var321, we evaluated a unique 5' allele identified in Proband 3 with primer set PROM2 (table S3). A single 4.7 kb fragment was amplified with Advantage 2 Polymerase Mix (BD Biosciences) to encompass the fragment containing both variant alleles, using PROM2 forward and 3' UTR2 reverse primers (table S3). Amplification proceeded with: Step 1:(1X) 95°C for 4 min; Step 2(30X) 95°C for 30 sec, 62°C for 30 sec, 72°C for 4 min; Step 3:(1X) 72°C for 10 min. The product was gel extracted, purified, and cloned with TOPO® XL PCR Cloning Kit (Invitrogen) per manufacturer's instructions. Clones were sequenced on both strands.

Sequencing Gel of Frameshift Variants

Frameshift variants were amplified with the following primers: F: GGATCTGGGCAACAATAACATC, R: GCGTGTCCAGGTAATTGCTATC. Each 10µl reaction contained: 200ng DNA template, 1µl 10X PCR Buffer, 1µl 100% DMSO, 1µl 1.25mM dNTP mix, 0.1µl ^{32}P dCTP, 0.1µl Taq DNA Polymerase, and 0.25µl 10µM of forward and reverse primer. Cycling parameters were as follows: Step 1:(1X) 94°C

for 3 min; Step 2:(35X) 95°C for 30 sec, 58°C for 30 sec, 72°C for 30 sec; Step 3:(1X) 72°C for 3 min. PCR products were analyzed using denaturing polyacrylamide gel electrophoresis.

SNP Genotyping

SNP genotyping was performed using the Sequenom MALDI-TOF MS system (*S3*). Primers for PCR amplification and primer extension reaction were designed using Spectrodesigner software (Sequenom, San Diego, CA) (table S5). PCR amplification was performed in 384-well plates. Each 5μl reaction contained 15ng DNA as template, 0.2μl $MgCl_2$, 0.5μl 10X PCR Buffer, 0.8μl dNTP, 0.02μl HotStar® Taq DNA polymerase (Qiagen Inc., Valencia, CA), and 0.075μl 4μM of forward and reverse primer (table S5). Cycling parameters were as follows: Step 1(1X) 95°C for 15 min; Step 2:(45X) 95°C for 20 sec, 56°C for 30 sec, 72°C for 60 sec; Step 3:(1X) 72°C for 3 min. PCR products were submitted to W.M. Keck Foundation Biotechnology Resource Laboratory for extension reaction and allele determination.

Human *SLITRK1* 3'UTR Luciferase and cDNA Constructs

The full-length 3' UTR of *SLITRK1* containing the wild type or var321 allele was amplified using forward primer TACTGGCACAATGGGCCTTAC and reverse primer CTGTCATGAAATGCAGTCCACA. The 3' UTR of Renilla luciferase in the vector pRL-SV40 (Promega, Madison, WI) was excised using restriction enzymes XbaI and

BamHI and replaced with the full-length 3'UTR of *SLITRK1*. The resulting constructs (pRL-wt *SLITRK*1-3'UTR and pRL-mut *SLITRK1*-3' UTR) were verified by sequencing.

Full length wild type and frameshift human *SLITRK1* were PCR amplified from control or patient samples. respectively, and cloned into a pCLEG plasmid. The resulting constructs were verified by direct sequencing.

Luciferase Assays

N2a cells were plated on poly-L-ornithine coated Costar® 24-well cell culture plates (Corning Inc., Acton, MA) at $5.0x10^5$ cells per well in DMEM supplemented with 10% fetal bovine serum and sodium pyruvate without antibiotics (Invitrogen). Four hours after plating, the cells were transfected with Lipofectamine 2000 (Invitrogen) using the manufacturer's protocol. In each well, 20.9 fmol of pRL-*SLITRK1*-3' UTR and 4.6 fmol of pGL3-control vector (Promega) were cotransfected with 20 pmol of hsa-miR-24-1 pre-miR or control pre-miR Neg-1 (Ambion, Austin, TX). Six replicates were performed for each treatment.

The dual-luciferase reporter assay (Promega) was used according to manufacturer's protocol. Twenty-four hours after transfection, cells in each well were lysed using 100 μl of passive lysis buffer and 20 μl of the lysate was used for the assay. Measurements were taken using the TD-20/20 luminometer (Turner Designs, Sunnyvale, CA).

Statistical analysis was performed for each quantity of miRNA using the non-parametric Mann-Whitney U test. Area-under-the-curve (AUC) for relative luciferase

ratios across each of the quantities of miRNA-189 was determined by summing the following formula across 6 replicates each at 4 different quantities of miRNA (20pmol, 5pmol, 1pmol, 0.2pmol) and was found to be significant ($p=0.002$) AUC = $15*0.5*(\text{luciferase}_{20pmol} + \text{luciferase}_{5pmol}) + 4*0.5*(\text{luciferase}_{5pmol} + \text{luciferase}_{1pmol}) + 0.8*0.5*(\text{luciferase}_{1pmol} + \text{luciferase}_{0.2pmol})$. The raw luciferase data are presented in table S8.

In Situ Hybridization

Experiments were carried out in accordance with an IACUC approved protocol at the Yale University School of Medicine. P9 and P14 mouse brains were fixed by intracardiac perfusion with 4% paraformaldehyde and sectioned at 36 μm using a sledge microtome. In situ hybridization of mouse and human brain tissue was performed as previously described with minor modifications (*S4*, *S5*). RNA probes complementary to mouse *Slitrk1* (bases 322 to 1383 of the mouse *Slitrk1* cDNA, NM_199065) were prepared and labeled with digoxigenin-11-UTP. The mouse *SLITRK1* sequence in the probe region is more than 90 percent identical to the human sequence.

To detect miR-189, a double-stranded template was generated by annealing two oligonucleotides (anti-sense miRNA-189: GTGCCTACTGAGCTGATATCAGTTTTCCTGTCTC; T7 promoter GTGCCTACTGAGCTGATATCAGTTTTCCTGTCTC) and filling in with Klenow. The miR-189 probe was prepared from this template and labeled with digoxigenin-11-UTP,

then purified by ethanol precipitation in the presence of 0.5 M ammonium acetate. In situ hybridization was performed as described (*S5*), except that the hybridization and subsequent washing steps were carried out at 46ºC, 22ºC below the predicted melting temperature of miR-189. Staining with NBT/BCIP was performed overnight at room temperature. Human fetal brain (20 w.g.) was obtained from Dr. Bradford Poulos at the Human Fetal Tissue Repository of the Albert Einstein College of Medicine under the guidelines approved by their Institutional Review Board.

In Utero Electroporation, Primary Neuronal Cell Cultures and Immunostaining

All surgeries were performed under sterile conditions as described (*S6*) and in accordance with an IACUC approved protocol at the Yale University School of Medicine. Briefly, pregnant mice 14.5 days post coitum (E14.5) were anesthetized with a Ketamine/Xylazine mixture. pCGLH plasmid was used to express GFP. Plasmid DNA containing Fast Green (10%, Sigma) was microinjected by pressure into the embryonic lateral ventricles using pulled glass pipettes (Sutter Instruments, Novato, CA) with a diameter of 25-50 μm. The DNA mixture (4 μg/μl, 1:4 ratio of *GFP*:*SLITRK1*) was electroporated into ventricular zone cells by discharging five electrical pulses of 41 V for 50 ms with a time interval of 950 ms via custom-made electrodes. Animals were sutured and left to survive for 24 hours. At E15.5, embryos were screened with a Zeiss Stemi SV11 fluorescent microscope (Zeiss, Inc., Thornwood, NY) and the ones expressing GFP were further processed for primary cortical neuronal cultures as described previously (*S7*). Cortical neurons were cultured at plating density of 75,000 cells/cm^2 on laminin/

poly-L-ornithine coated glass coverslips in 24-well plates. Cells were fixed with warm 4% paraformaldehyde at 2 days in vitro (DIV), 4 DIV and 6 DIV for 15 min and washed with PBS. Then cells were incubated for 45 min in blocking solution [5% Normal Donkey Serum (Jackson ImmunoResearch Laboratories, West Grove, PA), 1% Bovine Serum Albumin, 0.2% glycine, 0.2% lysine in 1xPBS]. After that, primary rabbit-anti-GFP (1:100; Invitrogen), secondary biotin-SP conjugated donkey anti-rabbit (1:250; Jackson ImmunoResearch Laboratories) and Vectastain ABC Elite kit complex (1:250; Vector Laboratories, Burlingame, CA) were respectively applied for 1 hour with 3x5 min washes using 1xPBS between the steps. Antibody binding was visualized with 3,3'-diaminobenzidine as a developing chromagen, 4 μl of 0.04% ammonium chloride, 0.5 μl of glucose oxidase type VII, and 10 μl of 0.05M nickel ammonium sulfate in 0.2M acetate buffer (pH 6). The peroxidase reaction was started by adding 20 μl of 10% (w/v) D-glucose. Sections were mounted in Cytoseal 60 (Richard-Allan Scientific, Kalamazoo, MI).

Quantitative Analysis of Dendrites

The quantitative analysis of dendritic growth was carried out in a blinded fashion such that neither the treatment condition nor the DIV stage were known to the person reconstructing the neurons. Only neurons with a pyramidal morphology and with readily distinguishable, unobstructed dendrites were analyzed. Twenty four to fifty GFP-immunopositive neurons within each condition (GFP, GFP+ wt *SLITRK1*, and GFP+ mut *SLITRK1*) and stage (2 DIV, 4 DIV and 6DIV) were reconstructed by 3D-stereological

reconstruction (a Zeiss Axioskop microscope with a motorized stage, 40x oil objective fitted with an Optronics camera, Goleta, CA) and analyzed using the Neurolucida 2000 software (Microbrightfield Inc., Williston, VT). The total dendritic length was averaged per cell (table S9). Statistical analysis was carried out using the 2-tailed Student's t-test with a significance level of $p<0.05$.

Fig. S1. Expression of *Slitrk1* mRNA and miR-189 in mouse brain. (**A** and **B**) In situ hybridization analysis of *Slitrk1* expression in the neocortex (Nctx) (A), cerebellum and brainstem (B), of a P14 mouse. *Slitrk1* is expressed in all layers of Nctx with highest expression in neurons of layer VI. In the cerebellum, *Slitrk1* is highly expressed in granule and Purkinje cells. In the brain stem, *Slitrk1* is expressed in the majority of nuclei. (**C** to **G**) In situ hybridization analysis of miR-189 expression in coronal sections of P14 (C and D) and P9 (E to G) mouse brains. (C) At P14, miR-189 is predominately expressed in layers II-IV of the primary somatosensory neocortex (D to F). Sporadic neurons in layer V also express miR-189. (D) Intense signal for miR-189 transcripts is present in the cerebellar granule cell layer, but not in the brain stem at P14. (E to G) At P9, miR-189 is widely expressed in the brain with highest expression in the neocortex (G), hippocampus, basal ganglia and thalamus (F). Red boxes in E denote areas enlarged in F and G. Scale bar, 60 μm (A, C, F and G), 700 μm (B and D), and 1 mm (E).

Fig. S1

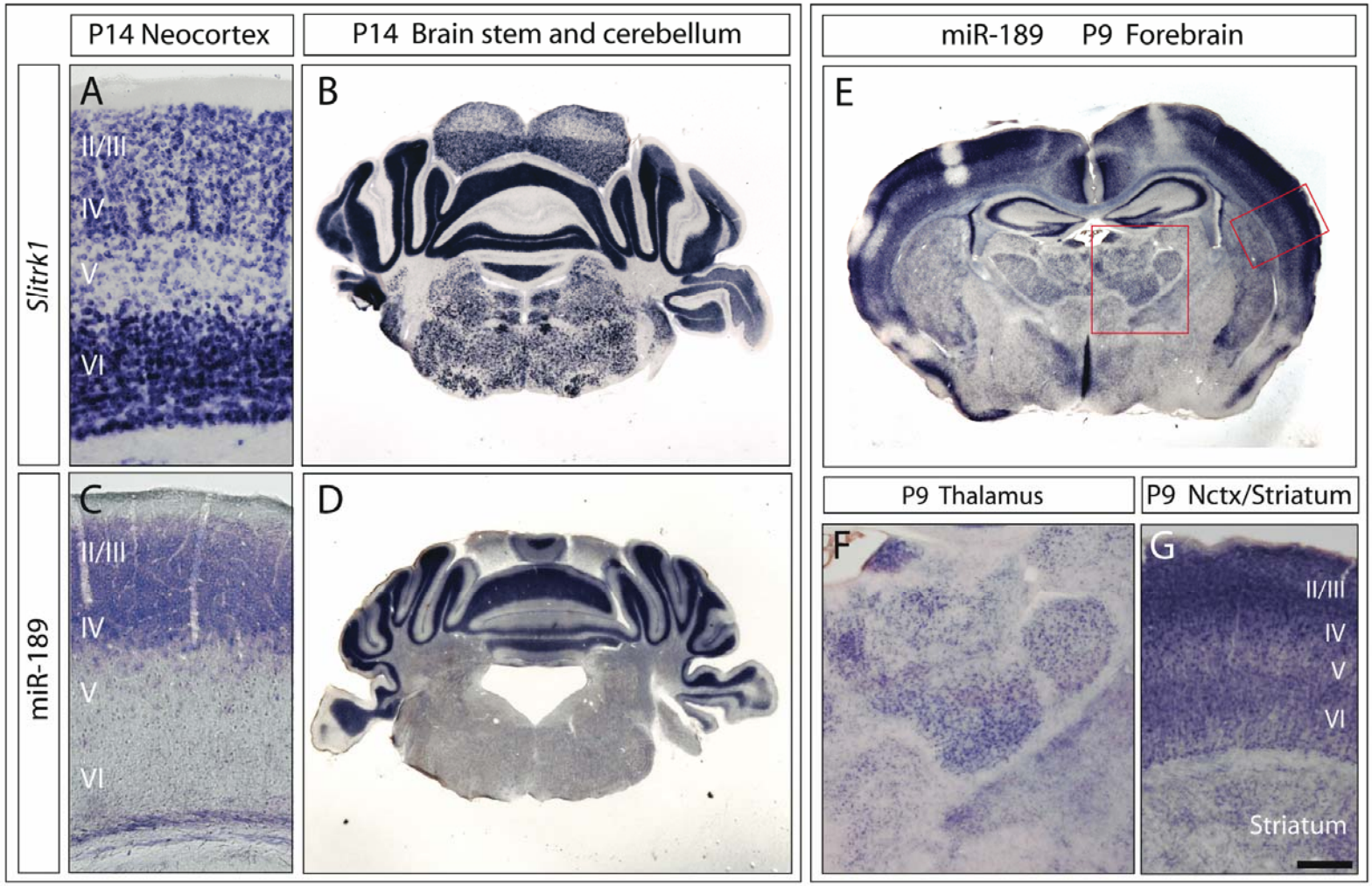
P14 Neocortex
P14 Brain stem and cerebellum
miR-189 P9 Forebrain
Slitrk1
miR-189
A
B
C
D
E
F
G
II/III
IV
V
VI
P9 Thalamus
P9 Nctx/Striatum
Striatum

Fig. S2. Expression of *SLITRK1* mRNA and miR-189 in fetal human brain at 20 w.g. (**A**) In situ hybridization of *SLITRK1* mRNA demonstrates expression in the neocortical plate (CP) and subplate (SP), putamen (Put) and globus pallidus (GP), thalamus (Th) and subthalamus (STh). (**B** and **C**) Higher magnification of the regions indicated by red boxes in (A) showing expression in STh (B) as well as in Put and in large neurons at the border of GP (C). (**D**) Expression of miR-189 in fetal human brain at 20 w.g. is detected in CP, SP, and intermediate zone (IZ). Scale bar 850 μm (A), 100 μm (B and C), and 350 μm (D).

Fig. S2

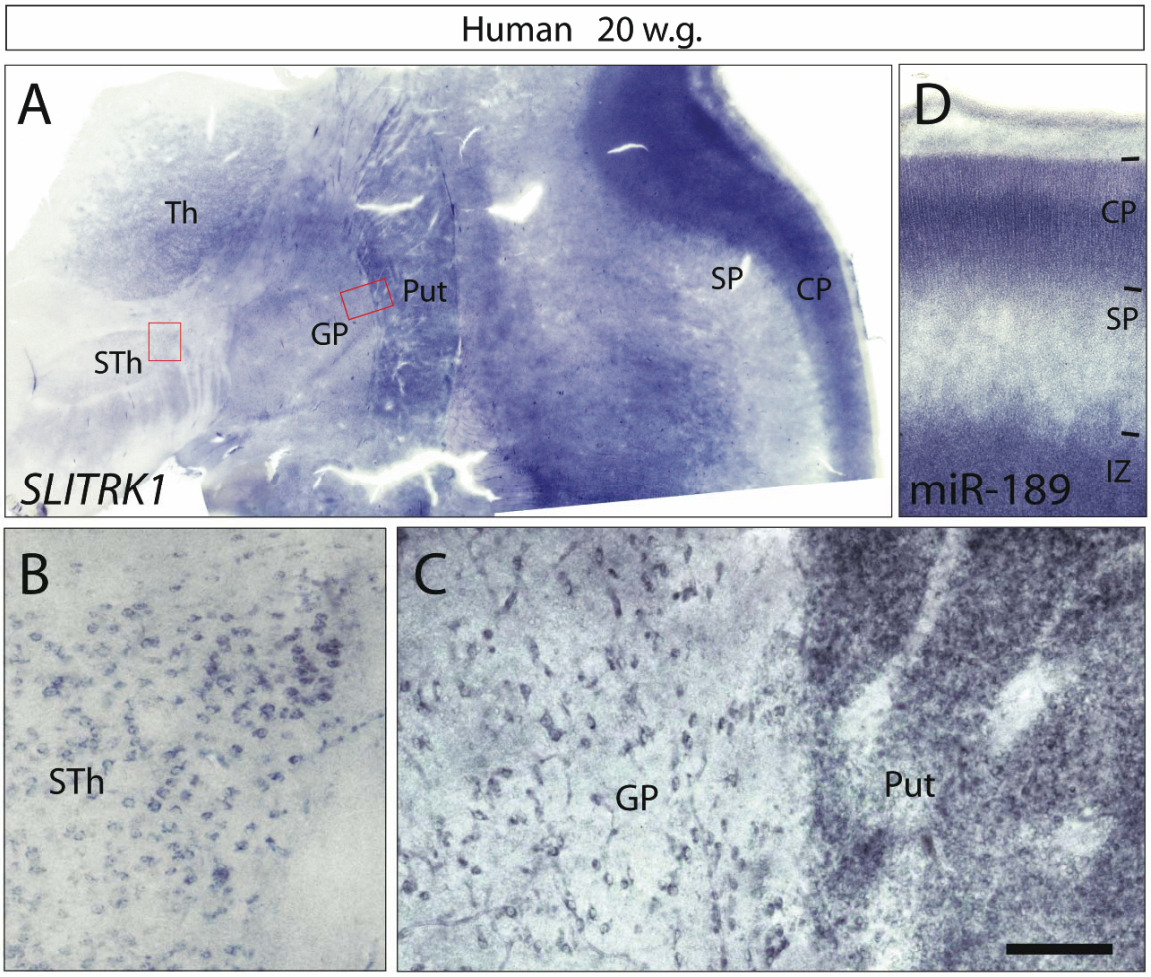
Human 20 w.g.
A
Th
Put
GP
SP
CP
STh
SLITRK1
D
CP
SP
IZ
miR-189
B
STh
C
GP
Put

Table S1. Markers used to confirm paternity in Families 1 and 4.

	Family 1			Family 4		
ABI Marker	**Father**	**Mother**	**Proband**	**Father**	**Mother**	**Proband**
D1S2800	0 , 1	0 , 1	1 , 1	0 , 1	0 , 2	0 , 0
D2S364	0 , 1	1 , 3	0 , 3	0 , 2	3 , 4	0 , 4
D2S367	0 , 5	1 , 3	0 , 3	2 , 4	3 , 4	2 , 4
D3S3681	1 , 2	2 , 3	2 , 2	2 , 2	0 , 0	0 , 2
D4S1534	2 , 5	0 , 4	4 , 5	1 , 1	1 , 3	1 , 1
D5S471	0 , 0	0 , 0	0 , 0	0 , 0	0 , 1	0 , 1
D6S422	0 , 0	1 , 2	0 , 1	1 , 1	1 , 1	1 , 1
D7S640	0 , 1	2 , 3	1 , 3	4 , 5	1 , 3	3 , 4
D8S272	1 , 3	0 , 5	1 , 5	1 , 4	1 , 2	2 , 4
D9S273	0 , 3	2 , 3	2 , 3	2 , 3	1 , 2	1 , 3
D10S212	2 , 2	1 , 4	1 , 2	0 , 2	0 , 3	0 , 2
D22S280	1 , 2	0 , 2	1 , 2	2 , 3	1 , 1	1 , 3

Table S2. BACs used in FISH mapping of inv(13)(q31;q33).

BAC ID	Base Position	Chromosomal Band	Position Relative to Break
RP11-428G23	chr13:76,620,410-76,745,373	13q22.3	Centromeric
RP11-52L5	chr13:77,954,915-78,112,216	13q31.1	Centromeric
RP11-173N7	chr13:78,550,587-78,696,802	13q31.1	Centromeric
RP11-470M1	chr13:79,425,661-79,586,247	13q31.1	Centromeric
RP11-521J24	chr13:80,495,762-80,694,720	13q31.1	Centromeric
RP11-115N13	chr13:82,035,430-82,201,311	13q31.1	Centromeric
RP11-400M8	chr13:82,201,212-82,280,653	13q31.1	Centromeric
RP11-49F20	chr13:82,278,654-82,413,998	13q31.1	Centromeric
RP11-89A14	chr13:82,411,999-82,577,009	13q31.1	Centromeric
RP11-464I4	chr13:82,592,802-82,779,067	13q31.1	Centromeric
RP11-635M6	chr13:82,851,010-82,999,627	13q31.1	Centromeric
RP11-375K12	chr13:82,916,224-83,126,061	13q31.1	Spanning
RP11-960P13	chr13:83,092,825-83,283,650	13q31.1	Telomeric
RP11-164B1	chr13:83,175,599-83,335,218	13q31.1	Telomeric
RP11-395N17	chr13:83,335,119-83,457,553	13q31.1	Telomeric
RP11-163N15	chr13:83,457,457-83,516,253	13q31.1	Telomeric
RP11-661D17	chr13:83,516,154-83,690,768	13q31.1	Telomeric
RP11-512M17	chr13:87,449,550-87,659,292	13q31.2	Telomeric
RP11-114G1	chr13:88,810,121-88,963,712	13q31.3	Telomeric
RP11-219C11	chr13:92,830,775-92,972,754	13q31.3	Telomeric
RP11-430M15	chr13:100,497,967-100,679,277	13q32.3-13q33.1	Centromeric
RP11-219L22	chr13:101,019,124-101,118,296	13q33.1	Centromeric
RP11-347N5	chr13:101,707,517-101,812,763	13q33.1	Centromeric
RP11-811P12	chr13:101,812,662-101,854,561	13q33.1	Centromeric
RP11-46I10	chr13:101,854,462-102,007,351	13q33.1	Centromeric
RP11-29B12	chr13:102,007,252-102,165,732	13q33.1	Centromeric
RP11-484I6	chr13:102,165,633-102,337,684	13q33.1	Centromeric
RP11-255P5	chr13:102,337,585-102,377,477	13q33.1	Spanning
RP11-11L8	chr13:102,377,378-102,548,509	13q33.1	Telomeric
RP11-260E14	chr13:102,548,410-102,712,470	13q33.1	Telomeric
RP11-78L19	chr13:103,576,237-103,757,777	13q33.1-13q33.2	Telomeric
RP11-562E17	chr13:104,304,190-104,442,099	13q33.2	Telomeric

Table S3. *SLITRK1* primer sequences and associated PCR amplification conditions.

Amplicon	Primers (Forward/Reverse)	Annealing Temperature (ºC)	PCR Cycles
PROM1	CATGTTCACGTTTTCTTCCATC	62	30
	GTATGTTCAAAGTGGCTTTCGG		
PROM2	CAAAGAACCTAACTCTCAATGACC	62	30
	AAAGATCTGACACCCTCTGCTG		
5'UTR1	TGTAGATCGTCAGCCTTTTATGC	55.8	35
	CGCTCTCGCTTACTAGCTCTTC		
5'UTR2	GAAATTTTCCAGCGCCATTG	63.3	35
	CCCCCACAACACTTTAAAAATAAC		
5'UTR3	CTTGCACTACGTGCCTGGATAG	TD*	TD*
	AGACGTCTCCAGCAACAGAATC		
CDS-1	TACTTTGTGATGAGATCGGGG	56.8	30
	AGCTTGTTCAAGTCCTGGAAGG		
CDS-2	GTGAAAAGGCTGCACATCAAC	56.8	30
	TTGAGGTCTTTACCCTGCAGTC		
CDS-3	GAGGAGGTCTTGGAGCAAATC	56.8	30
	GCAGTTCATCTTTAAACCCGAC		
CDS-4	AACTCCTTTCAAGACAAATGGG	56.8	30
	GAGCTGGATAGCGTTGTACTCC		
CDS-5	GTCGGGTTTAAAGATGAACTGC	56.8	30
	GATGATGGAGGTTAACTGGTCC		
CDS-6	CAACAACAACCTGCTGAGGTC	56.8	30
	GTTCCTCAGGATAAACACGAGC		
CDS-7	CAGCTGTACGCTAGGATCTCG	56.8	30
	TTGTTTCAAGGAGGGAGCTAAG		
3'UTR1	ACTCTTCCTACTGGCACAATGG	62	30
	ACGAGATGCCGTCTCCAGTC		
3'UTR2	AAAACAAAAAGTGCTGCATGG	62	30
	TTCCTCGGTTCTCTTTTCCTAC		
3'UTR3	CAATAATGCCTTCCATCTGAATG	58.9	35
	GGTAAAGTCTGAGCGAAGGTG		
3'UTR4	ATTTGCGGTGGAAGAGACAG	65	30
	AGGAGTGCTGACCAATGAAATC		
3'UTR5	CTCAGACTTTACCGGCTTTCC	TD*	TD*
	CATTGGTTCATAAAATTCGAACAG		
3'UTR6	TTGTTAAAGCACTCATCTTTATGG	63.3	30
	ATGGCCTTAGGAATAGTCATGG		
3'UTR7	GCAGTTGTAAGTAGATCTGCCATC	65	30
	AAGAAAAGTTCTCGCCTCTGTG		

* TD= touchdown protocol, refer to methods

Table S4. Variants identified in patients and controls.

Patient Coding Variants

Var	Position*	Sequence	AA Change	#Het
varCD011	195	CAGTTTTACCATTTATTTCT(G/A)CATGGCAATTCCCTCACTCG	Synonomous	1
varCD021	555	ATCACCCACCTCGACCTCCG(G/A)GGTAACAGGCTGAAAACGCT	Synonomous	1
varCD031	856	AGACCTTTGCTCCTGGACCC(C/T)TGCCAACTCCTTTCAAGACA	Synonomous	1
varCDfs	1264	AGAACAACACTTTCAAGAAC(C/)TTTTGGACCTCAGGTGGCTA	Frameshift	1

Control Coding Variants

Var	Position*	Sequence	AA Change	#Het
varCD012	139	TAGACTGTGAAAAAAAGGGC(T/C)TCACAAGTCTGCAGCGTTTC	F47L	1
varCD022	573	CGGGGTAACAGGCTGAAAAC(G/A)CTGCCCTATGAGGAGGTCTT	Synonomous	1
varCD061	1712	CTTTAGAAAGGATTTCATGC(T/C)CCTCTCCAATGACGAGATCT	L571P	1

Patient 3'UTR Variants

Var	Position*	Sequence	#Hom	#Het
var311	23	CCCCAACCCCAATAGGGGAG(G/A)GCAGAGGGAAGGCGATACAT	0	1
var321	689	TTTCGCCATTATTTGTGATC(G/A)GTAGGCAGTTCAGAGCATAA	0	2
rs9593836	801	GTTAACAATGTATTTTGTTG(A/C)GGGAAGTTTTTAGGGGTTGT	2	8
var331	1017	GACCAATTAATGTCACTCTA(G/A)TGCTTAGGCTGCGATCCTAT	0	2
rs3737193	1134	AATTCTATTCGAGGATTTTA(T/C)AATGGCATATTTTTTCAGTA	0	12
rs9602286	1160	CATATTTTTTCAGTATTAAA(G/A)CGAAAATGTTTTCAACTCTG	1	6
var341	1476	AAATGCAGCAGTGAATCCCT(T/C)TATTAATACTGGAAATCCCT	0	1
var351	1562	GATGTTAGGAGAGATTTGAT(T/A)TAATTGACTCTGCCTAGATA	0	10
var361, rs3164	2035-2043	TGCAGACTATAGATTTTTTT(TT/A/T)AATATAGGATTATAAATCAG		

*Position determined from RefSeq Gene *SLITRK1* : coding position from A in ATG start codon; 3'UTR position from first base after TAA stop codon. † Mutation screening analysis did not distinguish between the possible combinations of the three alleles. We sequenced 116 patients and found the following genotypes: 47 TT/TT, 8 TT/T, 51 TT/A, 2 T/T, 1 T/A, and 7 A/A. NOTE: We comprehensively screened 174 patients across the coding region and 139 patients across the 3'UTR. Hom=homozygous for minor allele.

Table S5. Primers used for Sequenom SNP genotyping assay of control samples.

Amplicon	Primers (Forward/Reverse)	Extension Primer	Extension 1	Extension 2
varCDfs	ACGTTGGATGCTGGGCAACAATAACATCGC ACGTTGGATGGCTATCCATGTATAGCCACC	CCACCTGAGGTCCAAAAG	CCACCTGAGGTCCAAAAGT	CCACCTGAGGTCCAAAAGGT
var321	ACGTTGGATGTCAGAAAGTGCCATTTCGCC ACGTTGGATGGACTAGCCATGCAAATGTCC	ATGCTCTGAACTGCCTAC	ATGCTCTGAACTGCCTACC	ATGCTCTGAACTGCCTACTG

Table S6. Predicted microRNA target sites in *SLITRK1* 3'UTR.

miRNA	Location*	Target Sequence	Source‡
miR-27a	115	GGCAUAAGUAGAUAAAUAACUGU	P
miR-27b	115	GGCAUAAGUAGAUAAAUAACUGU	P
miR-128b	118	AUAAGUAGAUAAAUAACUGUGA	P
miR-128a	118	AUAAGUAGAUAAAUAACUGUGA	P
miR-139	187	AAACAAAGAGCAGACUGUGGA	M
miR-27b	192	AAGAGCAGACUGUGGA	M
miR-297	341	UCUAUACAUAUAUACAUAUAU	M
miR-140	385	UAUCUAUUUUUCCCCUGUGGAU	M
miR-181b	447	CAGUUGCACGAAGGCAUGAAUGUA	M, T, P
miR-181a	448	AGUUGCACGAAGGCAUGAAUGUA	M, T, P
miR-181c	448	AGUUGCACGAAGGCAUGAAUGUA	M, T, P
miR-101	454	ACGAAGGCAUGAAUGUAUUGUA	M
miR-101b	454	ACGAAGGCAUGAAUGUAUUGUA	M
miR-15a	498	CAAAAAACAAAAAGUGCUGCAU	M
miR-15b	498	CAAAAAACAAAAAGUGCUGCAU	M
miR-183	648	CAGUAUAAUCAGAAAGUGCCAUU	M, T, P
miR-350	657	CAGAAAGUGCCAUUUCGCCAUUAUUUGUGAU	M
miR-24-1 (189)	**676**	**AUUAUUUGUGAUCGGUAGGCAG**	**M,P**
miR-27a	698	UUCAGAGCAUAAGUUAACUGU	P
miR-27b	698	UUCAGAGCAUAAGUUAACUGU	P
miR-128b	699	UCAGAGCAUAAGUUAACUGUGA	P
miR-128a	699	UCAGAGCAUAAGUUAACUGUGA	P
miR-193	741	UUAGGACAUUUGCAUGGCUAGUC	M
miR-33	775	UUAUGAGUUAACAAUGUAU	M
miR-190	878	GUCUUUUUUUUAAUACAUAUCC	T, P
miR-181c	902	UAAUGCCUUCCAUCUGAAUGUA	P
miR-181b	903	AAUGCCUUCCAUCUGAAUGUA	M, T, P
miR-369	928	AAGUACCCAUGAUUUCUAUUAUA	T
miR-141	934	CCAUGAUUUCUAUUAUAGUAUCA	T
miR-32	942	UCUAUUAUAGUAUCAGUGUAAUU	M
miR-15b	1037	UGGUAGCAAUUCUGUGCUGGUA	M, T
miR-195	1038	GGUAGCAAUUCUGUGCUGGUA	M, T
miR-362	1108	CUUACUAAUUCUAUUCGAGGAUU	M
miR-200b	1138	GGCAUAUUUUUUCAGUAUUA	T
miR-320	1179	UGGGUCCUUACCUUUUUCCAGCUUCA	M
miR-338	1460	GCAGCAGUGAAUCCCUUUAUUAAUACUGGA	M
miR-199b	1461	CAGCAGUGAAUCCCUUUAUUAAUACUGGA	M
miR-199a	1462	AGCAGUGAAUCCCUUUAUUAAUACUGGA	M
miR-145	1465	AGUGAAUCCCUUUAUUAAUACUGGAA	T
miR-29c	1499	CUGCUGCUUUUGUUGGUGCUG	M
miR-29a	1500	UGCUGCUUUUGUUGGUGCUGC	M
miR-17-3p	1513	GGUGCUGCCCACACUGCAGA	M, P
miR-223	1550	GAGAGAUUUGAUUUAAUUGACU	M
miR-345	1596	AGAGUGGAGAUUUCAUUGGUCAGCA	M
miR-295	1603	AGAUUUCAUUGGUCAGCACUCC	M
miR-15b	1640	CCUAAUGACUGGCAUUUGAGAUGCUGCUG	M
miR-29c	1645	UGACUGGCAUUUGAGAUGCUGCUG	M
miR-103/107	1645	UGACUGGCAUUUGAGAUGCUGCU	T
miR-15a	1646	GACUGGCAUUUGAGAUGCUGCUG	M
miR-195	1647	ACUGGCAUUUGAGAUGCUGCUG	M
miR-29b	1647	ACUGGCAUUUGAGAUGCUGCUG	M
miR-190	1974	AGUCUGCAUUCCACCACAUAUCC	P
miR-17-3p	2004	AGAAGUAUGUCAAAAGACUGCAGA	P
miR-352	2198	UAUUAUAAACCAUGACUAUUCC	M

*3'UTR position from first base after TAA stop codon. ‡Database sources: P=PicTar (http://pictar.bio.nyu.edu/), M=Human microRNA targets (http://www.microrna.org/), T=Targetscan (http://genes.mit.edu/targetscan/).

Table S7. Informative markers used to determine compatibility of var321 haplotypes.

				Genotypes				
	Marker	**Location**	**Distance from var321**	**Father 4**	**Mother 4**	**Proband 4**	**var321 Haplotype**	**Proband 3**
3'of *SLITRK1*	SL032	chr13:83,189,248-83,189,432	161,432	1 , 2	1 , 2	2 , 2	2	0 , 3
	SL031	chr13:83,267,306-83,267,344	83,520	0 , 0	0 , 1	0 , 1	1	0 , 0
	var321	chr13:83,350,864	0	0 , 0	0 , 1	0 , 1	1	0 , 1
5' of *SLITRK1*	var525	chr13:83,354,681	3,817	0 , 0	0 , 0	0 , 0	0	0 , 1*
	SL059	chr13:84,020,534-84,020,591	669,670	0 , 3	1 , 4	0 , 1	1	2 , 3

*It was determined by TOPO cloning that var321 is on same chromosome as var525 in Proband 3. Distances are in basepairs.

Table S8. Raw data and relative luciferase activity for luciferase reporter assay in N2a cells.

	miR-189						Ctrl-miR					
	wt *hSLITRK1* 3'UTR			mut *hSLITRK1* 3'UTR			wt *hSLITRK1* 3'UTR			mut *hSLITRK1* 3'UTR		
	Renilla	**Firefly**	**R/F**	**Renilla**	**Firefly**	**R/F**	**Renilla**	**Firefly**	**R/F**	**Renilla**	**Firefly**	**R/F**
20 pmol	267.8	145.2	0.5422	288.2	144.8	0.5024	523.5	931.8	1.780	530.3	923.2	1.741
	259.1	155.9	0.6017	291.0	145.5	0.5000	473.2	846.1	1.788	447.6	795.2	1.777
	231.0	135.5	0.5866	286.2	153.2	0.5353	385.7	719.4	1.865	506.0	917.1	1.812
	253.2	157.7	0.6228	251.1	134.2	0.5344	486.9	853.1	1.752	491.7	876.9	1.783
	263.3	161.7	0.6141	265.4	143.8	0.5418	472.5	917.7	1.942	457.7	813.4	1.777
	253.3	145.5	0.5744	303.2	157.1	0.5181	405.4	770.8	1.901	425.1	761.5	1.791
5 pmol	541.6	361.9	0.6682	437.4	269.4	0.6159	475.2	869.6	1.830	465.7	867.9	1.864
	451.9	322.0	0.7125	368.9	212.0	0.5747	500.6	973.0	1.944	501.3	882.9	1.761
	447.0	291.6	0.6523	476.7	301.2	0.6318	433.2	875.5	2.021	413.9	760.7	1.838
	421.3	292.9	0.6952	421.2	248.9	0.5909	392.5	763.7	1.946	542.4	1048.0	1.932
	393.6	250.4	0.6362	465.4	290.2	0.6235	516.3	1035.0	2.005	522.2	1033.0	1.978
	375.2	259.6	0.6919	451.4	300.1	0.6648	441.9	840.1	1.901	455.7	854.3	1.875
1 pmol	433.9	348.6	0.8034	425.7	269.0	0.6319	625.9	1154.0	1.844	588.9	1023.0	1.737
	360.8	283.2	0.7849	492.0	325.8	0.6622	529.1	984.8	1.861	559.2	969.0	1.733
	368.0	294.6	0.8005	471.1	312.5	0.6633	453.6	817.4	1.802	600.1	1028.0	1.713
	343.1	267.2	0.7788	530.3	336.8	0.6351	466.4	838.8	1.798	532.8	981.8	1.843
	368.7	286.9	0.7781	439.2	291.5	0.6637	483.1	912.3	1.888	560.5	1011.0	1.804
	491.7	415.5	0.8450	478.1	334.5	0.6996	424.2	754.0	1.777	572.9	1014.0	1.770
0.2 pmol	524.0	485.7	0.9269	577.3	498.2	0.8630	813.9	1165.0	1.431	631.0	918.1	1.455
	445.1	434.3	0.9757	471.0	387.2	0.8221	604.7	891.7	1.475	567.2	829.7	1.463
	400.5	352.6	0.8804	491.0	408.3	0.8316	589.4	874.2	1.483	710.7	1052.0	1.480
	473.1	430.0	0.9089	286.0	235.2	0.8224	592.5	898.0	1.516	613.9	926.0	1.508
	366.1	330.0	0.9014	559.4	465.3	0.8318	641.2	923.6	1.440	710.7	1087.0	1.529
	473.7	422.5	0.8919	510.7	410.7	0.8042	533.7	795.2	1.490	432.3	641.8	1.485

Relative luciferase activity is expressed as the Renilla to Firefly ratio (R/F).

Table S9. Mean ± SEM for Dendritic Growth in Primary Neuronal Cultures

	GFP	GFP + wt SLTRK1	GFP + mut SLITRK1
2 DIV	262.0 ± 6.387	312.1 ± 36.79	192.3 ± 9.969
4 DIV	635.4 ± 59.04	1045 ± 56.28	716.8 ± 82.62
6 DIV	1159 ± 66.39	2029 ± 174.1	1123 ± 164.7

DIV=days in vitro. All units μm.

Supporting References

S1. J. Knoll, P. Lichter in *Current Protocols in Human Genetics,* N. Dracopoli et al., Eds. (John Wiley and Sons, Inc., New York, 2005), pages 4.3.1-4.3.12

S2. M.W. Nachman, S.L. Crowell, *Genetics* **156**, 297 (2000).

S3. K. Nakai *et al*., *Hum. Mutat*. **20**, 133 (2002).

S4. E. A. Grove, S. Tole, J. Limon, L. Yip, C. W. Ragsdale, *Development* **125**, 2315 (1998).

S5. N. Šestan, P. Rakic, M. J. Donoghue, *Curr. Biol*. **11**, 39 (2001).

S6. T. Saito, N. Nakatsuji, *Dev. Biol.* **240**, 237 (2001).

S7. N. Šestan, S. Artavanis-Tsakonas, P. Rakic. *Science* **286**, 741 (1999).